Stem Cell Research (2014) 13, 390–403

Available online at www.sciencedirect.com

ScienceDirect

www.elsevier.com/locate/scr

METHODS AND REAGENTS

A PiggyBac-mediated approach for muscle gene transfer or cell therapy

Déborah Ley, Ruthger Van Zwieten [1], Stefania Puttini [1], Pavithra Iyer, Alessia Cochard, Nicolas Mermod*

Institute of Biotechnology, University of Lausanne and Center for Biotechnology UNIL-EPFL, Lausanne, Switzerland

Received 2 May 2014; received in revised form 27 August 2014; accepted 29 August 2014
Available online 8 September 2014

Abstract An emerging therapeutic approach for Duchenne muscular dystrophy is the transplantation of autologous myogenic progenitor cells genetically modified to express dystrophin. The use of this approach is challenged by the difficulty in maintaining these cells ex vivo while keeping their myogenic potential, and ensuring sufficient transgene expression following their transplantation and myogenic differentiation in vivo. We investigated the use of the *piggyBac* transposon system to achieve stable gene expression when transferred to cultured mesoangioblasts and into murine muscles. Without selection, up to 8% of the mesoangioblasts expressed the transgene from 1 to 2 genomic copies of the *piggyBac* vector. Integration occurred mostly in intergenic genomic DNA and transgene expression was stable in vitro. Intramuscular transplantation of mouse Tibialis anterior muscles with mesoangioblasts containing the transposon led to sustained myofiber GFP expression in vivo. In contrast, the direct electroporation of the transposon-donor plasmids in the mouse Tibialis muscles in vivo did not lead to sustained transgene expression despite molecular evidence of *piggyBac* transposition in vivo. Together these findings provide a proof-of-principle that *piggyBac* transposon may be considered for mesoangioblast cell-based therapies of muscular dystrophies.

Introduction

Duchenne muscular dystrophy (DMD) is characterized by a progressive muscle degeneration caused by mutations in one of the largest gene known, that of dystrophin (Koenig et al., 1987). There is no curative treatment at present and death usually occurs within 10 to 15 years of symptom onset, typically from breathing complications and cardiomyopathy (Emery, 1993). Current promising clinical and pre-clinical approaches include gene editing, exon skipping, gene therapy and stem cell therapies (Fairclough et al., 2013). Of these, exon skipping is currently most advanced, where the delivery or expression of small RNAs affecting splicing is used to remove a mutated dystrophin mRNA exon. However,

Abbreviations: CMV, cytomegalovirus; DMD, Duchenne muscular dystrophy; FACS, fluorescence-activated cell sorting; GAPDH, glyceraldehyde 3-phosphate dehydrogenase; GFP, green fluorescent protein; hMAR, human matrix attachment region; mdx, dystrophic; PB, *piggyBac*; PCR, polymerase chain reaction; PEI, polyethylenimine; Puro, puromycin resistance gene; qRT-PCR, quantitative real-time PCR; SCID, severe combined immunodeficiency; SEM, standard error of the mean; SV40, simian virus 40.

* Corresponding author at: Laboratory of Molecular Biotechnology, Station 6, EPFL, CH-1015 Lausanne, Switzerland. Fax: +41 21 693 76 10.
E-mail addresses: Deborah.Ley@unil.ch (D. Ley), ruthger.vanzwieten@unil.ch (R. Van Zwieten), stefania.puttini@epfl.ch (S. Puttini), Pavithra.iyer@unil.ch (P. Iyer), alessia.cochard@gmail.com (A. Cochard), Nicolas.Mermod@unil.ch (N. Mermod).
[1] These authors contributed equally to this work.

http://dx.doi.org/10.1016/j.scr.2014.08.007
1873-5061/

it may not offer a cure for all patients, depending on the type of the dystrophin gene mutation (Brolin and Shiraishi, 2011).

Other gene therapy strategies aim at the delivery of a functional dystrophin coding sequence into the dystrophic muscle of DMD patients. Viral vectors are commonly used in gene therapy for their efficient gene delivery and integration in the myofiber genomes, but their use may be limited to the expression of truncated dystrophin variants, due to cargo-size limitations of the viral capsid (Phelps et al., 1995; Duan et al., 1998). In addition, safety concerns were linked to malignant cell transformation due to insertional mutagenesis linked to certain viral vectors (Hacein-Bey-Abina et al., 2008; Lewinski and Bushman, 2005), whereas the immunogenicity of the viral particles is also a concern (Raper et al., 2003; Yei et al., 1994). Thus, alternatives to viral vector gene transfer are also currently assessed. For instance, an alternative gene transfer method is the in vivo electroporation of naked plasmids containing the dystrophin gene, which has little transgene size constraint and low immunogenicity. Plasmids or synthetic chromosomes can persist in the muscle fiber without genome integration and transgene expression can be relatively stable in the non-dividing myofibers (Puttini et al., 2009; Tedesco et al., 2011). However, the long-term expression of the transgene may be reduced by gradual silencing effects and/or by the loss of the episomal DNA.

Thus, the persistent muscle expression of full length dystrophin remains difficult to achieve currently. Since the discovery of satellite stem cells and the difficulties met in maintaining their differentiation potential during in vitro culture, several promising alternative candidates for DMD cell therapy have been identified. These include the blood vessel-associated mesoangioblast muscle precursor cells, as they are expandable in vitro and capable of systemic myogenic differentiation following intra-arterial injection (Cossu and Bianco, 2003). It was shown that mesoangioblasts from wild-type donors could restore functional and systemic dystrophin expression after intra-arterial transplantation in the golden retriever muscular dystrophy dog model, which led to increased life-span and improved muscle function and mobility (Sampaolesi et al., 2006). However, the outcome of the transfer of viral vector-transduced autologous cells expressing a truncated dystrophin was less encouraging.

One current challenge for the in vitro engineering of these cells using non-viral vectors is that they are difficult to transfect and have a limited expansion potential. Ideally, the complete dystrophin sequence should be stably integrated in low-copy number in non-coding sequences of the mesoangioblast genome, avoiding the mis-regulation of endogenous genes while allowing sufficient transgene expression to maintain efficacy. Transfer of the full-length dystrophin cDNA may be achieved via non-viral transfection methods that include chemical reagents and electroporation. However, the low transfection and integration rates and/or frequent transgene silencing of the non-viral vectors have limited progress for their use in mesoangioblasts (Tedesco et al., 2011; Murakami et al., 2003; Van Zwieten et al., submitted for publication; Yanagihara et al., 1996). The enrichment of a subpopulation of cells that display stable expression following transgene integration may thus be required, which is difficult to achieve using clinically acceptable practice, for instance because in vitro cell expansion can increase the likelihood of chromosomal rearrangement occurrence.

As a potential response to these issues, the *piggyBac* (PB) and *Sleeping Beauty* transposon systems may be proposed as alternatives, as they combine the relatively easier production of non-viral vectors with the efficient transgene integration and sustained expression in a broad variety of cell types (Ding et al., 2005; Handler et al., 1998; Ivics et al., 1997, 2009; Wilson et al., 2007). Among the known DNA transposons and integrating viral vectors, PB has the unique property to integrate cargos of up to 20 kb in mammalian cells without a significant loss of transposition efficiency (Ding et al., 2005). Moreover, PB has demonstrated its potential for gene or cell therapy applications, in particular in the context of difficult-to-transfect human embryonic stem cells or T-lymphocytes, and for the generation of induced pluripotent stem cells (Ding et al., 2005). Furthermore, incorporation of a epigenetic regulatory element, hMAR (human matrix attachment region) 1–68, in a PB transposon cassette, was shown to decrease silencing effect and to stabilize and increase transgene expression in cultured cell lines (Ley et al., 2013). However, the efficacy of PB transposon vectors has not been investigated in mesoangioblasts or in muscles in vivo.

Here, we addressed whether the use of PB vectors may allow stable transgene delivery and expression in mesoangioblasts following their transplantation into mouse muscles, and we assessed their performance relative to in vivo electroporation-mediated DNA delivery to mouse muscle. The PB vector was found to yield stable GFP expression in mesoangioblasts in culture as well as after their in vivo differentiation and fusion to myofibers following transplantation. The widespread expression observed from mesoangioblast transplantation was found to be persistent, unlike that obtained from the direct in situ muscle electroporation with the transposable vector DNA, despite the documented transposition events that occurred in vivo with this later approach. These findings indicated that PB vectors may provide a viable approach to achieve efficient and stable gene transfer in the context of DMD therapy.

Materials and methods

Plasmids and DNA vectors

The PB transposase expression vector pCS2+U5V5PBU3 containing the *PB* transposase coding sequence surrounded by the 5′ and 3′ untranslated terminal regions (UTR) of the *Xenopus laevis* β-globin gene (Fig. 1, left panel) was constructed as previously described (Ley et al., 2013). The different transposon vectors used in this study were generated by introducing the *PB* 235 bp 3′ and 310 bp 5′ inverted terminal repeats (ITRs) into the pBluescript SK-plasmid (Fig. 1, right panel). The MAR 1–68 element, the puromycin resistance and green fluorescent protein (GFP) genes used in this study were as previously described (Girod et al., 2007; Hart and Laemmli, 1998; Grandjean et al., 2011). The puromycin resistance gene (Puro) was under the control of the SV40 promoter originated from pRc/RSV

plasmid (Invitrogen/Life Technologies). The GFP protein was expressed using a eukaryotic expression cassette composed of a human cytomegalovirus (CMV) enhancer and human glyceraldehyde 3-phosphate dehydrogenase (GAPDH) promoter upstream of the coding sequence followed by a simian virus 40 (SV40) polyadenylation signal, the human gastrin terminator and a SV40 enhancer (Le Fourn et al., 2013). A DNA spacer of 3.6 kb corresponding to the MAR 1–68 length was polymerase chain reaction (PCR)-amplified from the mouse utrophin cDNA and used as control without MAR. The human GAPDH promoter was replaced by the SV40 promoter using standard cloning methods to assess GFP expression from a weak promoter in the context of transposable vectors (Fig. S3). Expression cassettes and/or MAR elements were inserted between the ITR sequences as illustrated in Fig. 1 using standard cloning methods.

Cell culture and transfections

The dystrophic (mdx) mesoangioblasts were kindly provided by G. Cossu and collaborators and cultivated in Dulbecco's modified eagle medium (DMEM, Gibco) containing 20% fetal bovine serum (FBS, Gibco) as previously described (Tonlorenzi et al., 2007). C2C12 mouse myoblasts were maintained in DMEM (Gibco) containing 10% FBS. For differentiation assay, mesoangioblasts and a 4-fold excess of C2C12 cells were co-cultured in DMEM for 24 h, after which cells were placed in differentiation medium, consisting of DMEM supplemented with 2% horse serum, for 5 days. Myofibers were fixed in 3% paraformaldehyde and immunostained with the primary mouse antibody anti-α-actinin (1:500, clone EA-53; Sigma) and secondary antibody Alexa Fluor 546-conjugated anti-mouse IgG (1:2000, Molecular Probes). Cell nuclei were counterstained with DAPI.

Transfections were performed using polyethylenimine (PEI) (JetPRIME, Polyplus Transfection) or Neon electroporation (Invitrogen) according to the manufacturer's instructions. For titration experiments using PEI, 150,000 cells were co-transfected with various amounts of circular PB transposase plasmid (ranging from 0 to 2.5 μg) and a fixed amount of 1.5 μg of circular transposon plasmid. For transposition experiments using PEI, 150,000 cells were co-transfected with 1 μg of circular PB transposase plasmid and 1.5 μg of circular transposon plasmids (optimal ratio of 1:1.5). For electroporations, 500,000 cells were co-transfected with 3 μg of circular transposase PB plasmid and 4.5 μg of circular transposon plasmid by two 1300 V pulses of 20 ms. For transposition experiments without selection, cells were passed every 2 days for 3 weeks in normal medium. For transposition experiment with selection, cells were placed in media containing 2 μg/ml puromycin 48 h after transfection and they were further cultured for 3 weeks. Cells were analyzed for GFP fluorescence by fluorescence-activated cell sorting (FACS) on day 2 after transfection to assess transient transfection efficiency analysis, and after 21 days of culture for transposition efficiency analysis. To determine the transgene copy number of unselected cells, stable GFP-expressing cells were sorted using a FACSAriaII. For GFP expression stability analysis, the percentage and fluorescence levels of GFP-positive sorted cells were followed by FACS for 1 month.

qPCR gene copy number assays

Genomic DNA was extracted and purified from unselected and selected stable GFP-expressing mesoangioblasts and Tibialis mouse muscles using the DNeasy Tissue Kit (Qiagen, Hilden, Germany) according to the manufacturer's protocol. Quantitative real-time PCR (qRT-PCR) relied on the SYBR Green-Taq polymerase kit from Eurogentec Inc. and ABI Prism 7700 PCR machine (Applied Biosystems), as adapted to estimate the number of genome-integrated transgene copies from 50 ng of genomic DNA. The GFP-Forward ACATTATG CCGGACAAAGCC and GFP-Reverse TTGTTTGGTAATGA TCA GCAAGTTG primers were used to amplify the GFP gene. The

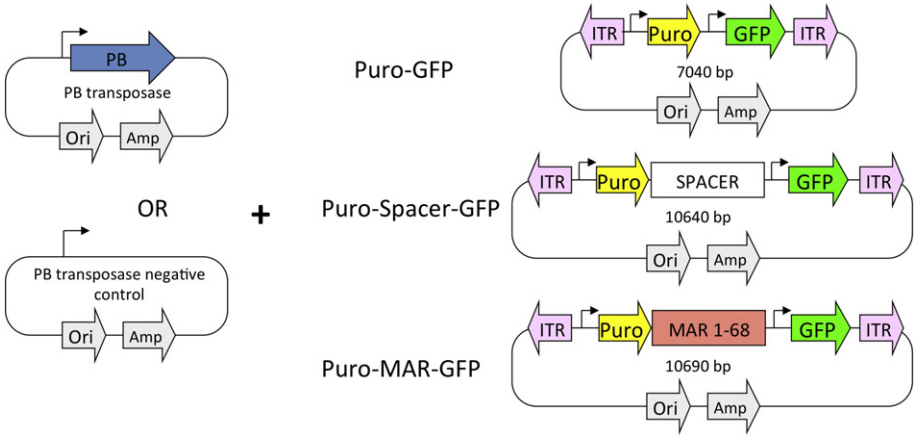

Figure 1 Overview of the PB expression constructs used in this study. The PB inverted terminal repeats (ITR), the PB transposase coding sequence (PB), the bacterial origin of replication (Ori) and the ampicillin selection gene (Amp) are schematically depicted on the plasmids used in this study. The puromycin resistance (Puro) and reporter green fluorescent protein (GFP) genes are illustrated by yellow and green arrows, and the spacer utrophin coding sequence and MAR 1–68 element are shown by white and red boxes, respectively, on the transposon donor plasmid derivatives.

M13-Forward TGTAAAACGACGGCCAGT and the M13-Reverse CAGGAAACAGCTATGACCATG primers were used to amplify excised plasmids for the transposon excision quantification assay. The Ftsj2-Forward GGGACCATCCATACCTTCG and Ftsj2-Reverse: GCTTGCTGGTGGTTTCCTC primers were used to amplify the Ftsj2 endogenous gene. The amplicon generated by the Ftsj2 primers gives one hit per haploid mouse genome using NCBI BLAST software. As mouse genome is diploid, we estimated that Ftsj2 is present at 2 copies per genome. The relative number of transgene copies per cell corresponded to the ratio between transgene and endogenous gene copies (Karlen et al., 2007).

Genomic integration site analysis and mapping

To determine the genomic integration sites of transfected mesoangioblasts and electroporated Tibialis mouse muscles, obtained as described in the "qPCR gene copy number assays" section above, we used the APAgeneTM GOLD Genome Walking kit to isolate unknown DNA sequences flanking known sequences, according to manufacturer's instruction. 3 specific primers were designed to anneal the end of the known 3′ ITR sequence for the nested PCR amplification steps, namely ACCGCATTGACAAGCACGCCTC AC, AGCGGCGACTGAGATGTCCTAAATG and CGACGGATTCGC GCTATTTAGAAAG in sequential order. The final PCR products were extracted from agarose gel and sequenced. Mapping of PB integration sites was performed using the UC Santa Cruz BLAT genome web-browser (mouse, December 2011 assembly). Only the sequencing results revealing an intact donor plasmid composed of the end of the 3′ ITR and a TTAA tetranucleotide marking the PB transposon border followed by a genomic sequence of at least 50 bp were taken into account. True PB integration sites were considered if the genomic sequence started immediately after the terminal TTAA at the end of the 3′ ITR sequence and matched at genomic locus with 95% identity. Distances of integration sites relative to gene on 5′ and 3′ side of the integration sites correspond to the distances between the stop codon of the downstream gene and between the ATG of the upstream gene and the integration site respectively (Figs. 4C and D).

Intramuscular mesoangioblast transplantation in nude mice

All animal experiments were done in accordance with institutional guidelines and authorizations for animal research by the State of Vaud veterinary office. In vivo experiments were done in 7-week-old CD1 nude mice (Charles River, USA). The wild-type mesoangioblasts were provided by G. Cossu and collaborators and cultivated as described in "Cell culture and transfection analysis" part. The Puro-GFP transposon and transposase plasmids were transfected in 1,000,000 mesoangioblasts per condition by NEON electroporation (Invitrogen) using the settings: 1300 V, 20 ms, and 2 pulses. Cells were co-transfected with 3 μg of transposase and 12 μg of transposon plasmids (ratio of 1:4) and a respective control in which the transposase plasmid was replaced by PB-devoid plasmid. All the cells were harvested 24 h after electroporation and 500,000 cells were resuspended in 25 μl PBS and transplanted into the Tibialis anterior muscle by intramuscular injection (3 muscles per time point, 1 injection trajectory per muscle). Tibialis anterior muscles were pre-injected with 25 μl cardiotoxin (10 μM) 24 h prior to transplantation of cells. 10, 30 and 60 days after transplantation, mice were sacrificed and the Tibialis anterior muscles were isolated.

Intramuscular electrotransfer of PB transposon in mice

In vivo electrotransfer was carried out on 5 week-old C57BL6 female mice (Iffa Credo-Charles River, France). Animals were housed in a facility with food and water ad libitum. The Tibialis anterior muscles were pre-treated with 0.8 U/μl of bovine hyaluronidase in 25 μl of normal saline 2–4 h before plasmid injection using a Hamilton syringe. Plasmid DNA in normal saline prepared by CsCl purification was injected intramuscularly. Four conditions were tested: 6 μg of the PB plasmid or control plasmid without transposase mixed with 20 μg of Puro-GFP or Puro-GFP-MAR transposon plasmids. All injections (30 μl) were carried out inside the Tibialis anterior muscle of four mice per condition, under Ketaminol (100 mg/kg) and Narcoxyl (75 mg/kg). Following the intramuscular injection of DNA, an electrical field of 200 V/cm in 8 ms pulses at 1 Hz (BTX electroporator) was applied to the muscle. Muscles were dissected after 7 days, 1 month and 9 months following electrotransfer.

Histochemical and quantification analysis of mouse muscles

Directly after dissection, GFP fluorescence in the whole Tibialis anterior muscle was observed by fluorescence microscopy. Then, muscles were embedded in gum tragacanth, frozen in isopentane at liquid nitrogen temperature, and stored at −80 °C for further analysis. 10 μm serial sections of the Tibialis muscles were prepared using a Cryostat at −25 °C. Sections were mounted onto glass slides and directly observed by fluorescence microscopy for GFP-positive myofiber analysis. To visualize the myofiber membranes, the sections were fixed in 3% paraformaldehyde and stained with Alexa594-conjugated agglutinin. For the assessment of tissue damage and morphology, sections were stained with hematoxylin–eosin, as described in Berry et al. (2007), and examined under a light microscope. All cells and tissues were visualized with a Zeiss microscope (Germany) and images were taken using an AxioCam MRm (Zeiss, Germany). Image processing and fluorescence quantification were performed with ImageJ software (NIH, USA).

Statistical analysis

The results are expressed as means ± standard error of the mean (SEM). "n" represents the number of individual experiments. Statistical analysis was performed using the two-tailed Student's t-test. Asterisks and crosses in the figure panels refer to statistical probabilities. Statistical probability values of less than 0.05 were considered significant.

Results

PB transposition efficiency in primary mesoangioblasts

PB-mediated gene transfer was shown to be functional in a range of cell lines (Ding et al., 2005; Chen et al., 2010; Nakazawa et al., 2009). However, PB transposon vectors have not been assessed in the context of primary muscle progenitor cells. To do so, we designed a series of transposon donor plasmids containing the Puro and the GFP reporter genes under the control of the SV40 promoter and strong CMV-GAPDH enhancer–promoter fusion, respectively, bracketed by the transposon ITRs (Fig. 1). To prevent potential chromatin-mediated silencing effects, the hMAR 1–68 or a control neutral spacer DNA sequence was inserted between the Puro and GFP genes, so as to investigate the effect of the MAR element on transposition efficiency and transgene expression independently of transposon size (Girod et al., 2007). As an excess or deficit of the PB transposase affects transposition efficiency (Grabundzija et al., 2010), we first evaluated transposition in response to varying ratios of the transposon donor plasmid and transposase expression vector following PEI mediated transfection. The transposition efficiency was determined from the number of GFP-expressing mesoangioblasts obtained with or without the expression of the PB transposase after three weeks of culture without selection following the transfection, to determine the optimal plasmid ratio, which was used in following assays (Fig. S1).

When using the Puro-GFP transposon and expressing the transposase, approximately 1% of the unselected cells maintained expression following PEI-mediated transfection (Fig. 2A). In contrast, gene transfer by electroporation yielded up to 8% of the mesoangioblasts stably expressing GFP in the mesoangioblast cell populations. The use of the larger transposons resulting from the inclusion of the spacer or hMAR 1–68 control resulted in a decreased proportion of GFP-expressing cells (51% and 39% respectively compared to that of the Puro-GFP vector), but still yielded around 3% of expressing cells upon the electroporation of the transposon donor and transposase expression plasmids. The number of mesoangioblasts stably expressing GFP from the Puro-Spacer and Puro-MAR transposon vectors was respectively 49% and 59% lower than that of the Puro-GFP vector, which paralleled well the transient GFP expression observed two days after gene transfer, implying that it is the DNA transfer efficacy that limits transposition success (Fig. S2). In the absence of the transposase, electroporation or PEI-mediated transfection yielded very low proportions of fluorescent

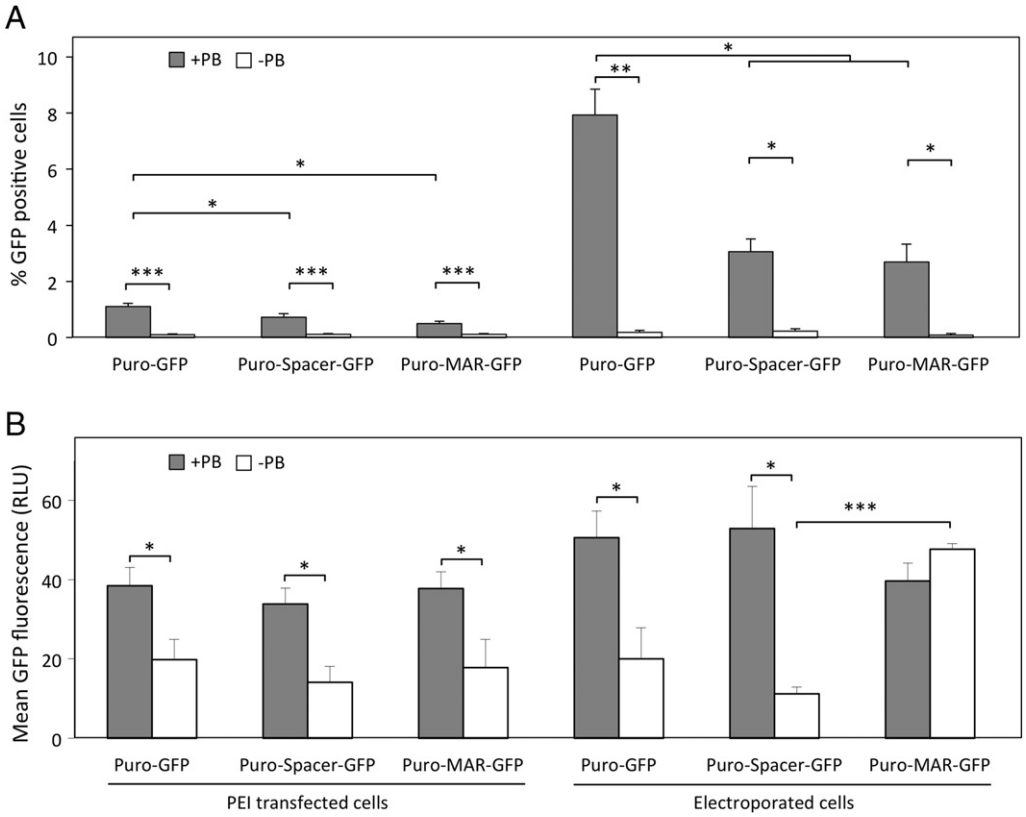

Figure 2 Transposition efficiency and expression from different transposon constructs and transfection methods. Mesoangioblasts were either transfected using PEI reagent or electroporated, with either the transposase expression vector (filled boxes) or with a negative control vector (open boxes), and with the Puro-GFP, Puro-Spacer-GFP or Puro-MAR-GFP transposon donor plasmid, as indicated. Cells were cultured without antibiotic selection for three weeks after transfection, and the percentage of GFP positive cells was determined by flow cytometry (A). Alternatively, the cells were sorted by cytofluorometry, and the fluorescence average was quantified from the polyclonal populations of GFP-expressing cells (B). Values represent the means ± SEM (n = 3; $*P < 0.05$; $**P < 0.01$; $***P < 0.001$).

cells, ranging between 0.1 and 0.2% (Fig. 2A). This indicated that spontaneous plasmid integration results from quite infrequent events in these primary cells.

Factors influencing expression from PB transposable vectors in mesoangioblasts

The GFP expression levels obtained by transposition or recombination events were quantified by flow cytometry assays of the stable mesoangioblast polyclonal populations. The fluorescence intensity of the GFP-expressing cells was similar for all conditions when the transposon donor plasmid was co-transfected with the transposase expression vector (Fig. 2B). Thus, the presence of the MAR or the size of the transposon did not affect the high expression levels obtained from the strong CMV enhancer and GAPDH promoter fusion upon transposition. However, when it was substituted by the relatively weaker SV40 promoter, the presence of the MAR increased both the occurrence of GFP-positive cells and their expression levels (Fig. S3). Upon the spontaneous plasmid integration observed without the transposase expression vector, the expression levels were also significantly increased by the inclusion of the MAR in electroporated plasmids, even when the strong CMV-GAPDH promoter was used (Figs. 2B and S4). Thus, we concluded that this MAR is functional in the context of transposable or plasmid vectors in primary mesoangioblasts. The MAR-mediated expression activation observed upon the use of a weaker promoter or upon spontaneous plasmid integration into the genome can be attributed to the known effects of this MAR to activate plasmid genomic integration by spontaneous recombination, to increase transgene transcription, and/or to suppress chromatin-mediated epigenetic silencing events linked to integration at unfavorable genomic loci (Grandjean et al., 2011; Galbete et al., 2009; Majocchi et al., 2014).

To distinguish the effects linked to transgene copy number variations from those elicited by changes in transgene transcription levels, we next assessed the copy number of the genome-integrated transposons in GFP-expressing cells. PB vector transposition led to the integration of 1 to 5 transgene copies on average in unselected mesoangioblasts (Fig. 3A). The copy number of spontaneously integrated plasmid copies was low upon PEI-mediated transfection or upon electroporation of the smaller plasmid, but the copy number was increased to 10 copies or more when the larger plasmids were electroporated in the absence of transposase. However, the expression levels were quite low despite the high transgene copy number, indicating that many of the transgenes were not expressed in a functional form (Fig. 3B). Indeed, the low level of expression per transgene copy may result from the DNA strand breaks caused by the electroporation of large plasmids, leading to the possible integration of

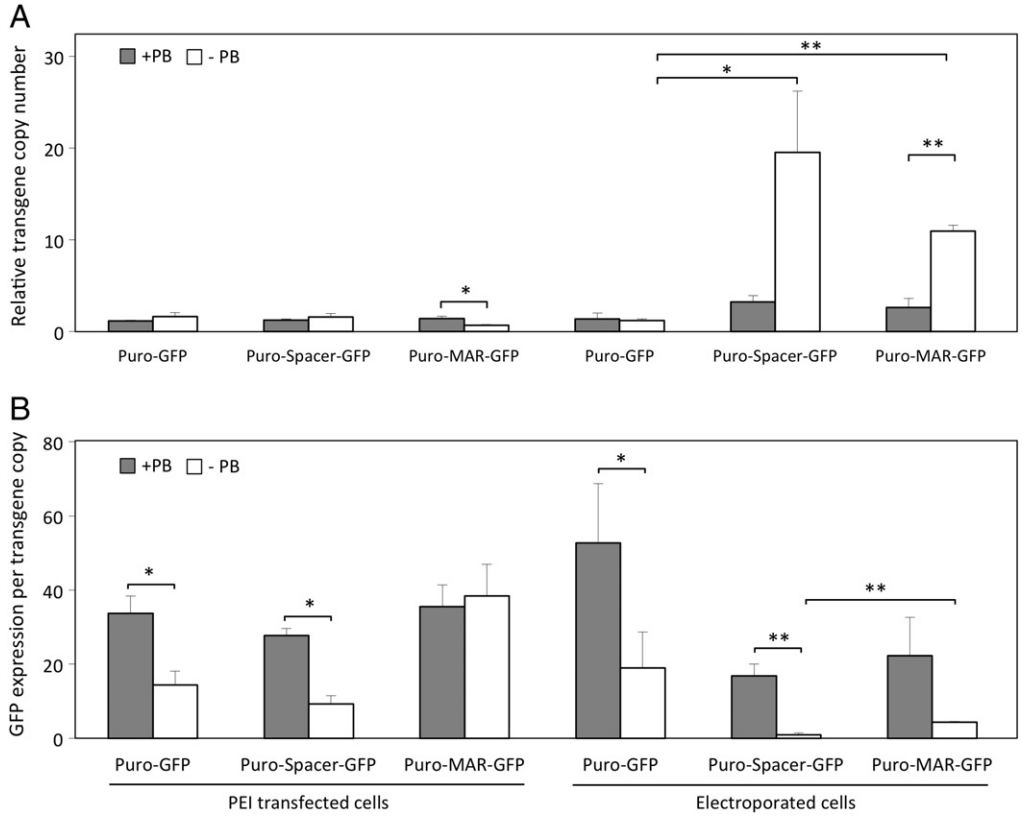

Figure 3 Transgene copy number and normalized expression in unselected mesoangioblasts. (A) The copy number of integrated GFP transgenes relative to those of the mouse genome FTSJ2 gene was determined using qPCR in unselected cells generated as described in Fig. 2B, following the cytofluorometric sorting of GFP-positive cells. (B) The mean fluorescence of the cell populations was divided by the number of integrated transgenes, so as to estimate the average expression per integrated GFP transgene copy. Values represent the means ± SEM (n = 3, $*P < 0.05$; $**P < 0.01$).

fragmented or damaged genes (Goldberg and Rubinsky, 2010). This mechanism also explains well the increased transgene copy number observed from the electroporation of large plasmids when compared to PEI transfection, as ruptured DNA strands promote the recombination of plasmids, which leads to concatemer formation, and their genomic integration (Grandjean et al., 2011). Nevertheless, expression of the transposase almost fully suppressed this effect, indicating that the transposase-mediated events predominate, as expected from the fact that spontaneous integration of functional transgenes is infrequent in these cells (Fig. 2A).

When the cells expressing the transgenes at the highest levels were selected by the addition of puromycin to the mesoangioblast cultures, higher transgene copy numbers were often observed in the absence of the transposase, when compared to non-selected cells (compare Figs. S4A and 3A). This is expected from the propensity of plasmids to form large concatemers before genomic integration by recombination, which usually results in the insertion of multiple plasmid copies within one integration locus (Folger et al., 1982; Hoglund et al., 1992). This was accompanied by increased expression levels from the MAR-containing plasmids, but not from the transposed vectors (Figs. S4B and S5). In contrast, the transgene copy number did not increase in selected cells relative to non-selected cells upon the transposition from the smaller Puro-GFP donor plasmid following electroporation (compare Figs. S4A and 3A). This indicated a homogeneously low number of integrated transposon copies in the unselected polyclonal cell population, as desired for a cell therapy use. Interestingly, the MAR did not increase the transgene copy number obtained from the spontaneous integration of plasmids in the genome of mesoangioblasts, in contrast to its effect to increase transgene copy number in transformed cell lines (Grandjean et al., 2011; Galbete et al., 2009). This likely reflects the low propensity of these primary cells to spontaneously recombine plasmid vectors into their genome, which is also a favorable property of the mesoangioblasts for therapeutic applications.

When the GFP expression was normalized to the transgene copy number, the highest expression level was obtained from the electroporation of the MAR or spacer-devoid Puro-GFP transposon in the presence of the transposase (Fig. 3B). This finding is consistent with previous proposals that transposable vectors have a propensity to integrate at genomic *loci* that are permissive for expression (Ley et al., 2013; Galvan et al., 2009; Matasci et al., 2011), where the presence of a MAR may be not needed. This also indicated that reliable transgene expression may be obtained by the integration of just 1–2 Puro-GFP transposon copies in the genome of mesoangioblasts. This conclusion was further supported by the assay of the GFP expression persistence from polyclonal mesoangioblast populations. After 1 month of culture without antibiotic selection, the percentage of GFP expressing cells and the fluorescence intensity remained highest from mesoangioblasts electroporated with the Puro-GFP transposable vector (Fig. S6). Overall, we therefore concluded that the use of the strong CMV-GAPDH promoter coupled to a PB transposon vector can fully alleviate the relatively low levels of expression that were observed upon spontaneous plasmid integration, and that reliable expression can be obtained in a high proportion of the primary cells from the use of this transposable vector.

PB integration site analysis in the mesoangioblasts

We next assessed the overall pattern of PB integration in the mesoangioblast genome. The transposon–genome junctions were PCR-amplified using ITR-specific and degenerate primers, followed by DNA sequencing (Lu et al., 2007). True transposition was distinguished from spontaneous integration events by the presence of the transposon ITR and of the characteristic TTAA sequence footprint marking the border between the transposon and the genome. This approach allowed the recovery of 22 distinct transposition events from various transposable vectors, which were mapped to the mouse genome (Fig. 4A). Distinct integration events were found in 12 chromosomes, often with multiple occurrences within the same chromosome, as illustrated by the 6 integrations located in distinct loci of chromosome 6.

We then examined the tendency of the PB transposon to integrate in genes or intergenic regions and if the type of transposable vector may influence the integration preference. A random pattern of integration should reflect the proportion of gene and non-gene DNA sequences present in the mouse genome, which was estimated to consist of approximately 70% of intergenic regions (Sakharkar et al., 2005). Overall, 73% of the retrieved transposon integrations were found in intergenic regions, and the highest proportion of intergenic inserts, over 85%, was obtained with the Puro-GFP transposon (Fig. 4B), implying that this transposon vector does not have a preference for integration in coding sequences. Of the 6 integration sites located within gene coding sequences, 5 occurred in intronic sequences and 1 in an exon–intron junction. To investigate if the transposons may integrate preferentially in regulatory regions located upstream of coding sequences such as promoters or enhancers, we plotted the occurrence of integration events relative to gene positions on either side of the integration sites. This indicated that most transposition events occurred at distances over 10 kb from the nearest coding sequence (Fig. 4C). Intergenic integration sites were mainly scattered beyond 10,000 bp and only one integration site was found within 1000 bp of an initiation site. However, when the occurrence of integration events was correlated to the interval length, the propensity of transposon insertion appeared to be highest within 10 kb of upstream sequences (Fig. 4D). This finding may in part explain the high and stable expression observed from few transposition events, given the known occurrence of a transcription-permissive chromatin structure on active and even inactive enhancers (Andersson et al., 2014). Overall, these findings are consistent with the lack of preferential transposon integration in coding sequences. Moreover, in the observed cases of transposition in the vicinity of genes, these results suggest a tropism for permissive chromatin environments such as those of upstream regulatory regions.

To further assess the number and the type of integration events, three GFP-positive mesoangioblast clones were randomly isolated and characterized for the transgene copy number, GFP expression and integration sites (Table 1). Two of the clones displayed a single transposon copy integrated at more than 100 kb of the nearest known gene, and they showed comparable GFP expression levels. The third clone revealed two different integration loci, one of which being within an intron, and it was found to express higher levels of

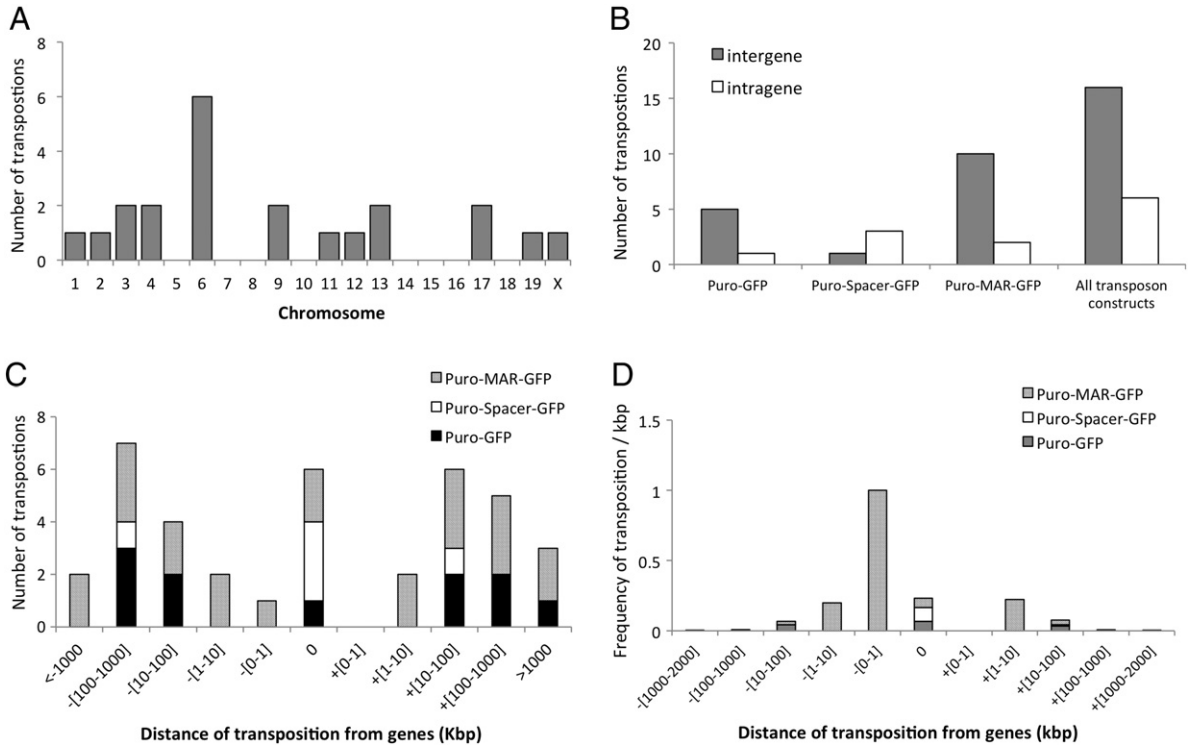

Figure 4 Sites of PB transposon integration preference in stable unselected GFP-expressing mesoangioblasts. 22 transposon integration sites were retrieved by chromosomal–transposon junction sequencing and mapped onto the mouse genome. (A) The number of PB integrations on each of the mouse chromosomes is shown. (B) Proportion of integration in genes or intergenic regions relative to the different transposon integration sites analyzed in this study. (C) Distribution of the transposon integration loci relative to the gene coding sequences on either side. The absolute numbers of integration events are given. (D) Frequency of transposition events relative to gene coding sequences. The number of integration events was normalized to 1000 bp windows, so as to estimate the propensity of transposons to integrate in coding and regulatory sequences or in intergenic regions irrespective of their relative size and proportion of the genome.

GFP. These results were consistent with those obtained from the analysis of polyclonal populations, and they demonstrated that sustained transgene expression could be readily obtained from a unique transposition event.

In vitro and in vivo differentiation of mesoangioblasts

An important key feature of mesoangioblasts is their ability to differentiate into myotubes in vitro, and into myofibers in vivo upon transplantation into muscles. Stable GFP-expressing polyclonal mesoangioblast populations obtained by PB transposition were first characterized using an in vitro differentiation assay. This consisted of co-culturing the mesoangioblasts with the C2C12 muscle progenitor cells under differentiation promoting conditions, where C2C12 cells form myotubes characterized by sarcomeric α-actinin expression (Fig. 5A). The presence of GFP-positive myotubes expressing sarcomeric α-actinin after co-culturing was indicative of mesoangioblast differentiation into myotubes and of the maintenance of GFP expression.

Table 1 PB vector integration site environment and expression in mesoangioblast cell clones.

Clone	Integration locus	Copy number	Integration features[a]	Distance from TSS[b]		Relative GFP fluorescence	
				At 5′	At 3′	RLU[c]	Per copy
C2	Chr9	1	Intergenic	−296,858	117,982	10	10
C3	Chr13	1	Intergenic	−70,000	50,000		
	Chr4	1	Intronic	–	–	65	37.5
C7	Chr6	1	Intergenic	−410,537	983,902	5	5

[a] Locations of insertion sites were determined using UCSC genome web-browser (mouse, December 2011 assembly).
[b] TSS: transcription start site.
[c] RLU: relative light unit.

We next tested the potential of mesoangioblasts to differentiate in vivo upon their transplantation in the Tibialis anterior muscle of immunodeficient nude mice one day after being electroporated with the Puro-GFP transposon vector. GFP expression was readily detected from whole muscles following the transplantation of mesoangioblasts electroporated with the Puro-GFP and PB transposase plasmids, and expression was maintained after one, two or six months (Fig. 5B). Muscle cross-sections revealed the fusion of the mesoangioblasts with the muscle fibers in vivo and persistent transgene expression, as illustrated by the strong cytosolic GFP signal displayed by the myofibers. In contrast, the GFP fluorescence was weaker in muscles transplanted with mesoangioblasts that were not electroporated with the transposase expression vector, where the fluorescence was confined to few muscle areas and was not stably maintained at the later time points. The proportion of GFP-positive myofibers was higher in muscles transplanted with mesoangioblasts transfected with the transposase expression plasmid at each time point, ranging from 10 to 50% of the myofibers in representative fluorescent areas, whereas cells transfected without the transposase yielded 1.5 to 25% of positive myofibers (Figs. S7 and S8). As the distribution of fluorescent myofibers was not homogeneous, we estimated the percentage of the fluorescent area over entire cross-sections along the muscles, to provide a more reliable and quantitative representation of the efficiency of the gene transfer approaches (Fig. 5C). Over 20% of the

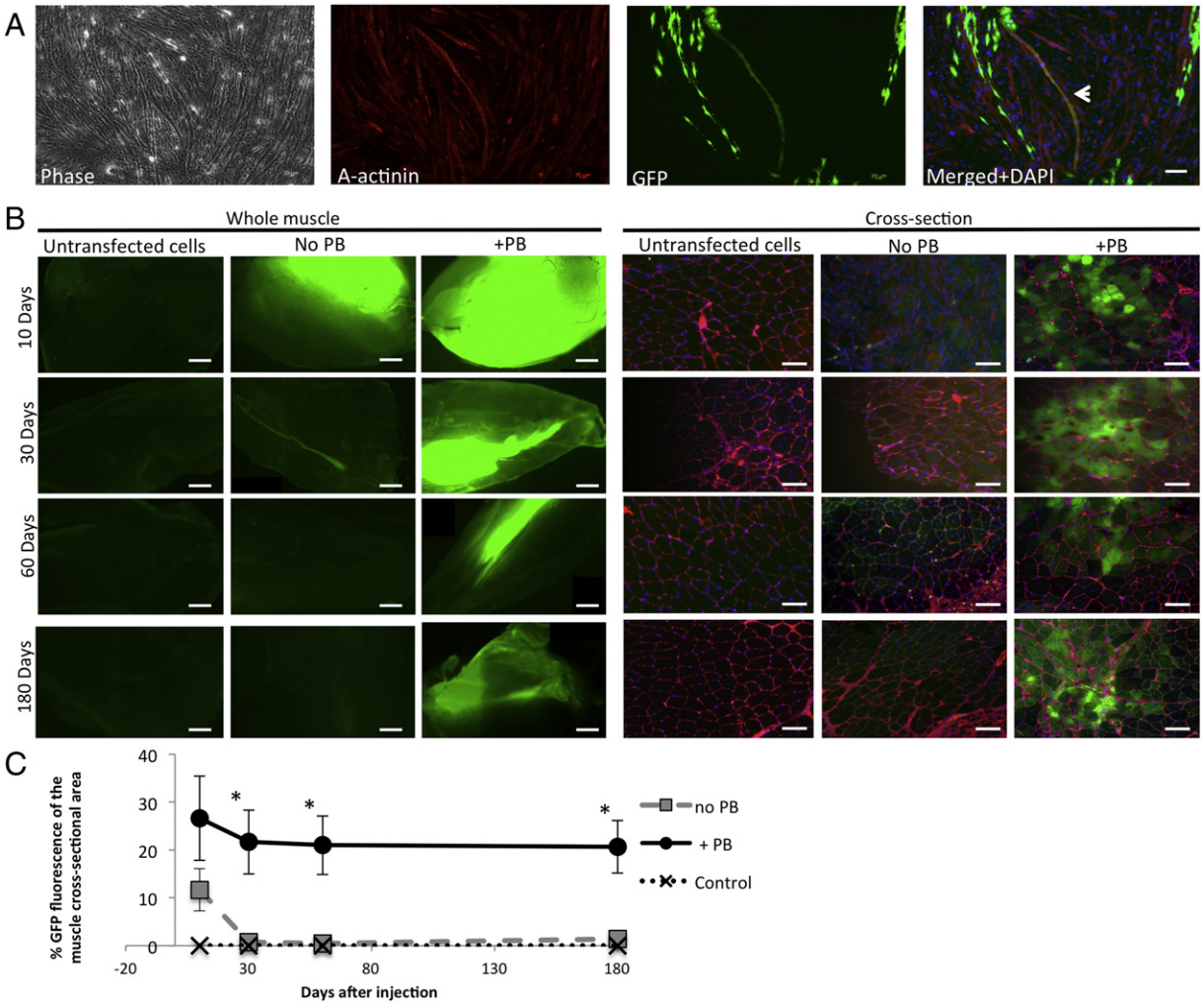

Figure 5 Mesoangioblast in vitro and in vivo differentiation assay. (A) Stable GFP-expressing mesoangioblasts obtained by transposition were co-cultured with C2C12 cells under low-serum differentiation-promoting conditions for five days. Nuclei were stained with DAPI. GFP-positive mesoangioblasts appear green. Myotubes immunostained for the presence of sarcomeric α-actinin appear in red. White arrow on the merged image shows GFP mesoangioblast fusion with C2C12 cells appearing in yellow. Scale bars = 50 μm. (B) Mesoangioblasts electroporated with the Puro-GFP transposon plasmid and the PB transposase (+PB) or empty control (no PB) plasmids were injected 24 h after in the Tibialis muscle of nude mice. GFP fluorescence of the whole (scale bars = 200 μm) and cross-section (scale bars = 50 μm) muscle is shown 10, 30, 60 and 180 days after injection. Sections were stained with Alexa594-conjugated agglutinin (red) to visualize the myofiber membranes. (C) GFP fluorescence areas of the entire muscle cross-section were quantified 10, 30, 60 and 180 days after injection. Values represent the means ± SEM (n = 2–3; *Indicates statistically significant differences between +PB and no PB groups; $P < 0.05$).

muscle area showed GFP fluorescence following the transplantation of cells transfected with the PB transposase vector after 6 months, corresponding to a 35-fold increase when compared to the muscles transplanted with mesoangioblasts devoid of the transposase, which was close to the background fluorescence of muscles injected with non-transfected mesoangioblasts. This suggested that transposition had occurred and that it led to the more sustained transgene expression.

Transposition of the Puro-GFP transposon vector in vivo was confirmed at the molecular level by the recovery of muscles and the determination of 10 genomic transposon integration sites by PCR amplification and DNA sequencing of the junctions of the vector ITR and cellular chromosomes (Table S1). 1 transposon had integrated in an exon, whereas 4 transposon integration events occurred in introns, revealing a possible increase of the frequency of integration within genes after transplantation when compared to the frequency found in transposed mesoangioblast in vitro (50% vs. 27%). Although these numbers do not allow definitive conclusions on the relative frequencies of genic integration, they nevertheless indicated that such events do occur from the transposable vectors, and they are reminiscent of several prior studies that reported different viral vector integration patterns before and after transduced cell transplantation (Ronen et al., 2011; Mantovani et al., 2009; Wang et al., 2009). Nevertheless, analysis of muscles dissected 2 months after the transplantation did not reveal any detectable cytotoxic effects, as observed from the quasi-absence of regenerating myofibers with central nuclei (Fig. S8), and they did not show any noticeable sign of inflammation, necrosis or tumor formation in any of the transplanted muscles.

The direct transfer of the transposon donor and transposase expression plasmids in the Tibialis muscles of healthy mice by intramuscular DNA injection and in vivo electroporation, termed electrotransfer, was also assessed for comparison with the mesoangioblast transplantation-based approach. One week after the electrotransfer, the explanted mice muscles expressed comparable GFP levels in about 20% of muscle fibers (Fig. 6). Muscles containing the GFP transposon donor plasmid but without the PB transposase displayed substantial levels of GFP over 250 days after the electrotransfer, and the proportion of GFP positive fibers was quite similar to that observed after 7 days. The maintenance of fluorescence at this time point is expected from the known persistence of episomal plasmids in the quiescent myofibers (Molnar et al., 2004; Stockdale and Holtzer, 1961), whereas expression of MAR-devoid plasmids usually decreases gradually thereafter (Puttini et al., 2013). However, in the presence of the transposase, the GFP fluorescence intensity unexpectedly decreased from the mouse muscles at a much faster pace, starting from 1 month post-electrotransfer to reach non-detectable levels at 9 months.

Potential toxic effects elicited by the electrotransfer of the PB transposase expression-vector were assessed from the occurrence of centrally nucleated muscle fibers, as a marker of regeneration resulting from myofiber damage. Centrally nucleated muscle fibers and cellular infiltrates were observed in muscles 1 month post-electrotransfer when compared to untreated controls (Fig. S9), which may result from muscle damages resulting from the electroporation process, as documented previously (Hartikka et al., 2001). However, inclusion of the transposase vector did not increase significantly the number of centrally nucleated muscle fibers or of cellular infiltrates when compared to muscles containing the transposase sequence-devoid control plasmid.

Persistence of the PB transposase plasmid in the myofibers was explored by qPCR analysis (Fig. S10A). The PB transposase plasmid was detected 7 days after electroporation and it decreased close to the background signal obtained without DNA electrotransfer after 1 month. Similar observations were obtained from the electrotransfer of the muscles of dystrophin-devoid mdx mice that may be more prone to muscle fiber degeneration. Finally, the PB transposase activity in myofibers was assessed by means of its transposon excision and integration properties. After excision of the transposon, the linear donor plasmid can be religated by cellular DNA repair activities, yielding a shorter product upon PCR amplification (Mitra et al., 2008). Excised products were detected in mice electroporated with the PB transposase plasmid, revealing that the PB transposase was active in myofibers in vivo (Fig. S10B). This was confirmed by the DNA sequencing of 4 transposon–genome junction events, providing direct evidence of PB transposition (Table S1). Overall, these findings indicated that the PB transposase was functional in myofibers, that its expression was not associated to detectable toxic effects, and that it mediated transposon vector integration into the multinucleated muscle fibers' genome from direct plasmid electrotransfer, despite the observed gradual loss of expression.

Taken together, these results indicated that the PB vector was capable of mediating persistent transgene expression in undifferentiated mesoangioblasts in vitro as well as in differentiated muscle fibers upon their transplantation in vivo. They also showed that stable and wide areas of expression can be obtained from the transplantation of mesoangioblasts electroporated with transposon vectors in vitro, as opposed to the direct in vivo electroporation of the transposon vector. Finally, mesoangioblast transplantation was not accompanied by the signs of myofiber damage and inflammation elicited by plasmid electrotransfer, which should be of advantage when considering the transplantation of diseased muscles as in the Duchenne muscular dystrophy.

Discussion

Several prior studies reported on the successful isolation of mesoangioblasts, their in vitro culture, and the maintenance of their potential to differentiate into myotubes (Farini et al., 2009). The transplantation of wild-type mesoangioblasts was shown to improve significantly muscle function in canine models of Duchene muscular dystrophy (Sampaolesi et al., 2006; Galvez et al., 2006). However, the transplantation of allogeneic healthy mesoangioblasts requires a continued immunosuppressive therapy, whereas the expression of dystrophin in autologous dystrophic mesoangioblasts using viral vectors displayed modest therapeutic benefits. Thus, the development of gene therapies for myopathies by autologous cell transplantation remains challenged by current gene transfer approaches, which have either a low

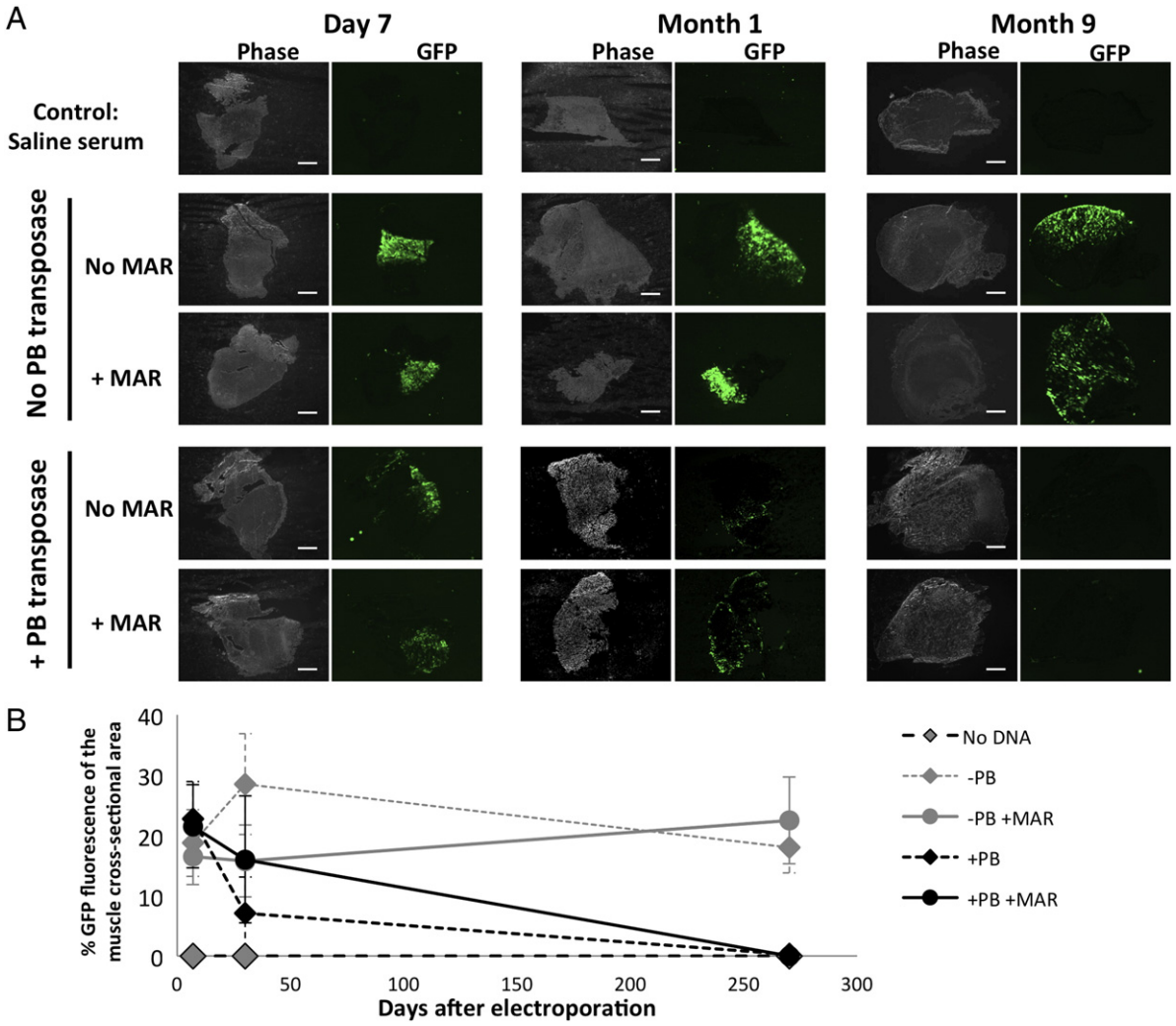

Figure 6 GFP fluorescence from direct PB transposon electrotransfer in Tibialis mouse muscles. The MAR containing or MAR devoid transposon donor plasmid was introduced with or without the PB transposase expression vector, as indicated, in murine Tibialis anterior muscles by direct electrotransfer of the plasmid DNA. GFP fluorescence in cross section of mouse muscles (A), and the mean percentage of GFP fluorescence of cross-sectional area (B), were determined at different time points following the electrotransfer, as for Fig. 5 (n = 4). Scale bars = 500 μm.

efficacy for large coding sequences or result in the expression of truncated dystrophin derivatives. Here, we assessed the potential benefit of using PB transposon vectors for sustained transgene expression in cultured mesoangioblasts and upon their differentiation into muscle fibers following transplantation.

We show that the PB transposon and its transposase are functional and quite efficient in terms of stable gene transfer to primary mesoangioblasts when compared to the transfection of plasmid vectors. Transposition occurred even when using large transposons comprising two expression cassettes and a spacer or MAR element. The decrease of transposition efficiency observed with the larger transposons was paralleled by the lower transient transfection efficiency of the larger plasmids. This may therefore result from the known lower efficiency of the transfer of larger plasmids, which was previously shown to be inversely proportional to the size of the transfected DNA (Kreiss et al., 1999). This negative effect of large cargo DNA was reduced when using electroporation, a method that confers high transient expression but that may result in a lower frequency of integration of functional transgene copies. Here we show that the electroporation of the larger plasmids may lead to reduced expression despite the integration of many and probably often non-functional transgene copies in the absence of the transposase. However, expression of the transposase and vector transposition yielded low and homogenous copy numbers of well-expressed transgenes, and thus it nearly abolished these unwanted effects while allowing expression in 3–8% of the total cell population in the absence of any selection. Thus, transposition remained efficient in primary mesoangioblasts even when using transposons over 11 kb, in agreement with studies performed on other types of undifferentiated primary cells (Ding et al., 2005).

This study also shows that transposition can lead to higher expression levels per integrated transgene copy when compared to spontaneous plasmid integration, and that this high

and persistent expression is mediated by few transposition events. Inclusion of a MAR element to reduce silencing effects was not accompanied by higher or more sustained expression in mesoangioblasts when placed next to potent promoter and enhancer sequences within the transposon vector, which contrasts with its requirement to achieve maximal transgene expression in cultured cell lines (Ley et al., 2013). This might reflect the less prominent silencing effects of undifferentiated primary cells, or a different tropism of the PB transposase in terms of the chromatin structure of the targeted genomic DNA in these cells.

The PB transposase was proposed to preferentially integrate single copies of the transposon at genomic *loci* with a chromatin structure that is permissive for expression, whereas spontaneous plasmid integration occurs from rare recombination events of multiple copies of concatemerized plasmids with the cell genome, increasing the probability of transgene silencing (Folger et al., 1982; McBurney et al., 2002). The integration of a high number of plasmid copies was especially prominent following the antibiotic selection of cells having integrated plasmids in their genome by spontaneous recombination, as surviving clones expressing the antibiotic resistance gene often possessed a high plasmid copy number. This was not observed with the PB transposon vector, where the number of transgene copies remained within 1–3 copies, even following antibiotic selection, indicating a homogeneously low number of integrated transposon in the unselected polyclonal cell population.

The propensity of some gene therapy viral vectors to integrate near the promoter or within the transcribed portion of cellular genes has been well documented (Gabriel et al., 2012; Nowrouzi et al., 2012). Whether the PB transposon may integrate preferentially at or near transcription units has also been the subject of several studies, and a preferential integration within or near transcribed genes has also been observed in some of the studies, although it may be influenced by the cell type and/or from biases introduced by the selection of cells expressing high levels of an antibiotic resistance gene (Wilson et al., 2007; Galvan et al., 2009; Huang et al., 2010). Here we found that the transposition of PB vectors may not occur preferentially in the genes of unselected mesoangioblast populations, since 73% of the recovered integration events were found in intergenic regions, mainly beyond 10 kb from the nearest transcribed gene sequence, although genic integration events were also observed. Furthermore, we demonstrated the feasibility of obtaining mesoangioblast clonal populations expressing GFP at stable levels from a single intergenic transposon integration site. These stable mesoangioblast clones maintained their ability to differentiate in vivo and to mediate GFP expression. These findings support the rationale of using PB transposon vectors to develop stem cell based therapeutic approaches.

Finally, we provide molecular evidence for PB transposase activity in vivo after plasmid intramuscular injection and electrotransfer of the murine muscles, for instance from the recovery and sequencing of several transposon–genomic junctions. Interestingly, such integration events were not able to mediate sustained transgene expression, as the GFP fluorescence declined for the muscles electroporated with the PB transposase expression vector. In contrast, GFP expression was more stable when the electrotransfer was performed in the absence of the transposase, which has been associated with the spontaneous genomic integration of episomal plasmid vectors in prior studies (Puttini et al., 2013). The cause of the lack of persistent expression from in vivo electroporated transposable vectors in the presence of the transposase remains unclear at present. It may include the persistence of low levels of the episomal transposase vector, leading to the remobilization of the transposons until they would either integrate into repressive chromatin structure or be lost from abortive transposition events. Alternatively, toxicity resulting from the persistent expression of the transposase episomal expression plasmid cannot be fully excluded, even if no signs of myofiber necrosis or regeneration were observed.

The loss of expression was nevertheless not observed from the transplantation of mesoangioblasts first electroporated with the transposon donor plasmid and transposase expression vector in vitro, followed by their transplantation in vivo. Thus, transposition in dividing mesoangioblasts allowed sustained expression in vivo, even after their transplantation and differentiation to fuse with resident myofibers. Overall, this study thus provides a first proof-of-principle of the feasibility of gene transfer mediated by transposon vectors in mesoangioblasts in vitro and in myofibers in vivo. The PB transposon vectors may offer several advantages for gene transfer over other non-viral or plasmid-based methods, such as a higher frequency of cells stably expressing the cargo gene without the need of antibiotic selection, and/or a lower propensity to epigenetic silencing effects. Relative to viral vectors, the PB transposon allows the efficient integration of larger transgenes in undifferentiated and myofiber-differentiated mesoangioblasts, providing a rationale for the assay of PB transposon vectors to achieve stable dystrophin transfer in animal models of Duchenne muscular dystrophy.

Acknowledgments

This work was supported by grants of the Commission for Technology and Innovation of the Swiss Confederation and Selexis SA, the European Union Clinigene Network of Excellence in gene therapy and by the University of Lausanne. The funders had no role in study design, data collection and analysis, decision to publish, or preparation of the manuscript.

Author contributions

Conceived and designed the experiments: NM, DL, SP, RVZ. Performed the experiments: DL, SP, RVZ, PI. Analyzed the data: DL, SP, RVZ, PI, NM. Wrote the paper: DL, NM.

Appendix A. Supplementary data

Supplementary data to this article can be found online at http://dx.doi.org/10.1016/j.scr.2014.08.007.

References

Andersson, R., Gebhard, C., Miguel-Escalada, I., Hoof, I., Bornholdt, J., Boyd, M., Chen, Y., Zhao, X., Schmidl, C., Suzuki, T., et al., 2014. An atlas of active enhancers across human cell types and tissues. Nature 507, 455–461.

Berry, S.E., Liu, J., Chaney, E.J., Kaufman, S.J., 2007. Multipotential mesoangioblast stem cell therapy in the mdx/utrn−/− mouse model for Duchenne muscular dystrophy. Regen. Med. 2, 275–288.

Brolin, C., Shiraishi, T., 2011. Antisense mediated exon skipping therapy for Duchenne muscular dystrophy (DMD). Artif. DNA PNA XNA 2, 6–15.

Chen, Y.T., Furushima, K., Hou, P.S., Ku, A.T., Deng, J.M., Jang, C.W., Fang, H., Adams, H.P., Kuo, M.L., Ho, H.N., et al., 2010. PiggyBac transposon-mediated, reversible gene transfer in human embryonic stem cells. Stem Cells Dev. 19, 763–771.

Cossu, G., Bianco, P., 2003. Mesoangioblasts—vascular progenitors for extravascular mesodermal tissues. Curr. Opin. Genet. Dev. 13, 537–542.

Ding, S., Wu, X., Li, G., Han, M., Zhuang, Y., Xu, T., 2005. Efficient transposition of the piggyBac (PB) transposon in mammalian cells and mice. Cell 122, 473–483.

Duan, D., Sharma, P., Yang, J., Yue, Y., Dudus, L., Zhang, Y., Fisher, K.J., Engelhardt, J.F., 1998. Circular intermediates of recombinant adeno-associated virus have defined structural characteristics responsible for long-term episomal persistence in muscle tissue. J. Virol. 72, 8568–8577.

Emery, A.E., 1993. Duchenne muscular dystrophy—Meryon's disease. Neuromuscul. Disord. 3, 263–266.

Fairclough, R.J., Wood, M.J., Davies, K.E., 2013. Therapy for Duchenne muscular dystrophy: renewed optimism from genetic approaches. Nat. Rev. Genet. 14, 373–378.

Farini, A., Razini, P., Erratico, S., Torrente, Y., Meregalli, M., 2009. Cell based therapy for Duchenne muscular dystrophy. J. Cell. Physiol. 221, 526–534.

Folger, K.R., Wong, E.A., Wahl, G., Capecchi, M.R., 1982. Patterns of integration of DNA microinjected into cultured mammalian cells: evidence for homologous recombination between injected plasmid DNA molecules. Mol. Cell. Biol. 2, 1372–1387.

Gabriel, R., Schmidt, M., von Kalle, C., 2012. Integration of retroviral vectors. Curr. Opin. Immunol. 24, 592–597.

Galbete, J.L., Buceta, M., Mermod, N., 2009. MAR elements regulate the probability of epigenetic switching between active and inactive gene expression. Mol. Biosyst. 5, 143–150.

Galvan, D.L., Nakazawa, Y., Kaja, A., Kettlun, C., Cooper, L.J., Rooney, C.M., Wilson, M.H., 2009. Genome-wide mapping of PiggyBac transposon integrations in primary human T cells. J. Immunother. 32, 837–844.

Galvez, B.G., Sampaolesi, M., Brunelli, S., Covarello, D., Gavina, M., Rossi, B., Constantin, G., Torrente, Y., Cossu, G., 2006. Complete repair of dystrophic skeletal muscle by mesoangioblasts with enhanced migration ability. J. Cell Biol. 174, 231–243.

Girod, P.A., Nguyen, D.Q., Calabrese, D., Puttini, S., Grandjean, M., Martinet, D., Regamey, A., Saugy, D., Beckmann, J.S., Bucher, P., Mermod, N., 2007. Genome-wide prediction of matrix attachment regions that increase gene expression in mammalian cells. Nat. Methods 4, 747–753.

Goldberg, A., Rubinsky, B., 2010. The effect of electroporation type pulsed electric fields on DNA in aqueous solution. Technol. Cancer Res. Treat. 9, 423–430.

Grabundzija, I., Irgang, M., Mates, L., Belay, E., Matrai, J., Gogol-Doring, A., Kawakami, K., Chen, W., Ruiz, P., Chuah, M.K., et al., 2010. Comparative analysis of transposable element vector systems in human cells. Mol. Ther. 18, 1200–1209.

Grandjean, M., Girod, P.A., Calabrese, D., Kostyrko, K., Wicht, M., Yerly, F., Mazza, C., Beckmann, J.S., Martinet, D., Mermod, N., 2011. High-level transgene expression by homologous recombination-mediated gene transfer. Nucleic Acids Res. 39, e104.

Hacein-Bey-Abina, S., Garrigue, A., Wang, G.P., Soulier, J., Lim, A., Morillon, E., Clappier, E., Caccavelli, L., Delabesse, E., Beldjord, K., et al., 2008. Insertional oncogenesis in 4 patients after retrovirus-mediated gene therapy of SCID-X1. J. Clin. Invest. 118, 3132–3142.

Handler, A.M., McCombs, S.D., Fraser, M.J., Saul, S.H., 1998. The lepidopteran transposon vector, piggyBac, mediates germ-line transformation in the Mediterranean fruit fly. Proc. Natl. Acad. Sci. U. S. A. 95, 7520–7525.

Hart, C.M., Laemmli, U.K., 1998. Facilitation of chromatin dynamics by SARs. Curr. Opin. Genet. Dev. 8, 519–525.

Hartikka, J., Sukhu, L., Buchner, C., Hazard, D., Bozoukova, V., Margalith, M., Nishioka, W.K., Wheeler, C.J., Manthorp, M., Sawdey, M., 2001. Electroporation-facilitated delivery of plasmid DNA in skeletal muscle: plasmid dependence of muscle damage and effect of poloxamer 188. Mol. Ther. 4, 407–415.

Hoglund, M., Siden, T., Rohme, D., 1992. Different pathways for chromosomal integration of transfected circular pSVneo plasmids in normal and established rodent cells. Gene 116, 215–222.

Huang, X., Guo, H., Tammana, S., Jung, Y.C., Mellgren, E., Bassi, P., Cao, Q., Tu, Z.J., Kim, Y.C., Ekker, S.C., et al., 2010. Gene transfer efficiency and genome-wide integration profiling of Sleeping Beauty, Tol2, and piggyBac transposons in human primary T cells. Mol. Ther. 18, 1803–1813.

Ivics, Z., Hackett, P.B., Plasterk, R.H., Izsvak, Z., 1997. Molecular reconstruction of Sleeping Beauty, a Tc1-like transposon from fish, and its transposition in human cells. Cell 91, 501–510.

Ivics, Z., Li, M.A., Mates, L., Boeke, J.D., Nagy, A., Bradley, A., Izsvak, Z., 2009. Transposon-mediated genome manipulation in vertebrates. Nat. Methods 6, 415–422.

Karlen, Y., McNair, A., Perseguers, S., Mazza, C., Mermod, N., 2007. Statistical significance of quantitative PCR. BMC Bioinformatics 8, 131.

Koenig, M., Hoffman, E.P., Bertelson, C.J., Monaco, A.P., Feener, C., Kunkel, L.M., 1987. Complete cloning of the Duchenne muscular dystrophy (DMD) cDNA and preliminary genomic organization of the DMD gene in normal and affected individuals. Cell 50, 509–517.

Kreiss, P., Cameron, B., Rangara, R., Mailhe, P., Aguerre-Charriol, O., Airiau, M., Scherman, D., Crouzet, J., Pitard, B., 1999. Plasmid DNA size does not affect the physicochemical properties of lipoplexes but modulates gene transfer efficiency. Nucleic Acids Res. 27, 3792–3798.

Le Fourn, V., Girod, P.A., Buceta, M., Regamey, A., Mermod, N., 2013. CHO cell engineering to prevent polypeptide aggregation and improve therapeutic protein secretion. Metab. Eng. 21, 91–102.

Lewinski, M.K., Bushman, F.D., 2005. Retroviral DNA integration—mechanism and consequences. Adv. Genet. 55, 147–181.

Ley, D., Harraghy, N., Le Fourn, V., Bire, S., Girod, P.A., Regamey, A., Rouleux-Bonnin, F., Bigot, Y., Mermod, N., 2013. MAR elements and transposons for improved transgene integration and expression. PLoS One 8, e62784.

Lu, B., Geurts, A.M., Poirier, C., Petit, D.C., Harrison, W., Overbeek, P.A., Bishop, C.E., 2007. Generation of rat mutants using a coat color-tagged Sleeping Beauty transposon system. Mamm. Genome 18, 338–346.

Majocchi, S., Aritonovska, E., Mermod, N., 2014. Epigenetic regulatory elements associate with specific histone modifications to prevent silencing of telomeric genes. Nucleic Acids Res. 42, 193–204.

Mantovani, J., Charrier, S., Eckenberg, R., Saurin, W., Danos, O., Perea, J., Galy, A., 2009. Diverse genomic integration of a lentiviral vector developed for the treatment of Wiskott–Aldrich syndrome. J. Gene Med. 11, 645–654.

Matasci, M., Baldi, L., Hacker, D.L., Wurm, F.M., 2011. The PiggyBac transposon enhances the frequency of CHO stable cell line generation and yields recombinant lines with superior productivity and stability. Biotechnol. Bioeng. 108, 2141–2150.

McBurney, M.W., Mai, T., Yang, X., Jardine, K., 2002. Evidence for repeat-induced gene silencing in cultured mammalian cells: inactivation of tandem repeats of transfected genes. Exp. Cell Res. 274, 1–8.

Mitra, R., Fain-Thornton, J., Craig, N.L., 2008. piggyBac can bypass DNA synthesis during cut and paste transposition. EMBO J. 27, 1097–1109.

Molnar, M.J., Gilbert, R., Lu, Y., Liu, A.B., Guo, A., Larochelle, N., Orlopp, K., Lochmuller, H., Petrof, B.J., Nalbantoglu, J., Karpati, G., 2004. Factors influencing the efficacy, longevity, and safety of electroporation-assisted plasmid-based gene transfer into mouse muscles. Mol. Ther. 10, 447–455.

Murakami, T., Nishi, T., Kimura, E., Goto, T., Maeda, Y., Ushio, Y., Uchino, M., Sunada, Y., 2003. Full-length dystrophin cDNA transfer into skeletal muscle of adult mdx mice by electroporation. Muscle Nerve 27, 237–241.

Nakazawa, Y., Huye, L.E., Dotti, G., Foster, A.E., Vera, J.F., Manuri, P.R., June, C.H., Rooney, C.M., Wilson, M.H., 2009. Optimization of the PiggyBac transposon system for the sustained genetic modification of human T lymphocytes. J. Immunother. 32, 826–836.

Nowrouzi, A., Penaud-Budloo, M., Kaeppel, C., Appelt, U., Le Guiner, C., Moullier, P., von Kalle, C., Snyder, R.O., Schmidt, M., 2012. Integration frequency and intermolecular recombination of rAAV vectors in non-human primate skeletal muscle and liver. Mol. Ther. 20, 1177–1186.

Phelps, S.F., Hauser, M.A., Cole, N.M., Rafael, J.A., Hinkle, R.T., Faulkner, J.A., Chamberlain, J.S., 1995. Expression of full-length and truncated dystrophin mini-genes in transgenic mdx mice. Hum. Mol. Genet. 4, 1251–1258.

Puttini, S., Lekka, M., Dorchies, O.M., Saugy, D., Incitti, T., Ruegg, U.T., Bozzoni, I., Kulik, A.J., Mermod, N., 2009. Gene-mediated restoration of normal myofiber elasticity in dystrophic muscles. Mol. Ther. 17, 19–25.

Puttini, S., van Zwieten, R.W., Saugy, D., Lekka, M.G., Hogger, F., Ley, D., Kulik, A.J., Mermod, N., 2013. MAR-mediated integration of plasmid vectors for in vivo gene transfer and regulation. BMC Mol. Biol. 14, 26.

Raper, S.E., Chirmule, N., Lee, F.S., Wivel, N.A., Bagg, A., Gao, G.P., Wilson, J.M., Batshaw, M.L., 2003. Fatal systemic inflammatory response syndrome in a ornithine transcarbamylase deficient patient following adenoviral gene transfer. Mol. Genet. Metab. 80, 148–158.

Ronen, K., Negre, O., Roth, S., Colomb, C., Malani, N., Denaro, M., Brady, T., Fusil, F., Gillet-Legrand, B., Hehir, K., et al., 2011. Distribution of lentiviral vector integration sites in mice following therapeutic gene transfer to treat beta-thalassemia. Mol. Ther. 19, 1273–1286.

Sakharkar, M.K., Perumal, B.S., Sakharkar, K.R., Kangueane, P., 2005. An analysis on gene architecture in human and mouse genomes. In Silico Biol. 5, 347–365.

Sampaolesi, M., Blot, S., D'Antona, G., Granger, N., Tonlorenzi, R., Innocenzi, A., Mognol, P., Thibaud, J.L., Galvez, B.G., Barthelemy, I., et al., 2006. Mesoangioblast stem cells ameliorate muscle function in dystrophic dogs. Nature 444, 574–579.

Stockdale, F.E., Holtzer, H., 1961. DNA synthesis and myogenesis. Exp. Cell Res. 24, 508–520.

Tedesco, F.S., Hoshiya, H., D'Antona, G., Gerli, M.F., Messina, G., Antonini, S., Tonlorenzi, R., Benedetti, S., Berghella, L., Torrente, Y., et al., 2011. Stem cell-mediated transfer of a human artificial chromosome ameliorates muscular dystrophy. Sci. Transl. Med. 3, 96ra78.

Tonlorenzi, R., Dellavalle, A., Schnapp, E., Cossu, G., Sampaolesi, M., 2007. Isolation and characterization of mesoangioblasts from mouse, dog, and human tissues. Curr. Protoc. Stem Cell Biol. 2B1, 1–29.

Van Zwieten, R.M.S., Puttini, S., Messina, G., Tedesco, F.S., Cossu, G., Mermod, N., 2014. MAR-mediated Dystrophin Expression in Mesoangioblasts for Duchenne Muscular Dystrophy Cell Therapy, (submitted for publication).

Wang, G.P., Levine, B.L., Binder, G.K., Berry, C.C., Malani, N., McGarrity, G., Tebas, P., June, C.H., Bushman, F.D., 2009. Analysis of lentiviral vector integration in HIV+ study subjects receiving autologous infusions of gene modified CD4+ T cells. Mol. Ther. 17, 844–850.

Wilson, M.H., Coates, C.J., George Jr., A.L., 2007. PiggyBac transposon-mediated gene transfer in human cells. Mol. Ther. 15, 139–145.

Yanagihara, I., Inui, K., Dickson, G., Turner, G., Piper, T., Kaneda, Y., Okada, S., 1996. Expression of full-length human dystrophin cDNA in mdx mouse muscle by HVJ-liposome injection. Gene Ther. 3, 549–553.

Yei, S., Mittereder, N., Tang, K., O'Sullivan, C., Trapnell, B.C., 1994. Adenovirus-mediated gene transfer for cystic fibrosis: quantitative evaluation of repeated in vivo vector administration to the lung. Gene Ther. 1, 192–200.